# Cx26 regulates proliferation of repairing basal airway epithelial cells

Crespin, Sophie; Bacchetta, Marc; Bou Saab, Joanna; Tantilipikorn, P; Bellec, J; Dudez, Tecla; Nguyen, T H; Kwak, Brenda; Lacroix, Jean-Sylvain; Huang, S; Wiszniewski, Ludovic; Chanson, Marc

**How to cite**

CRESPIN, Sophie et al. Cx26 regulates proliferation of repairing basal airway epithelial cells. In: International journal of biochemistry & cell biology, 2014, vol. 52, p. 152–160. doi: 10.1016/j.biocel.2014.02.010

This publication URL: https://archive-ouverte.unige.ch/unige:36912

Publication DOI: 10.1016/j.biocel.2014.02.010

# Cx26 regulates proliferation of repairing basal airway epithelial cells

Crespin S[a], Bacchetta M[a], Bou Saab J[a], Tantilipikorn P[b], Bellec J[c], Dudez T[a], Nguyen T[c], Kwak BR[d], Lacroix JS[e], Huang S[f], Wiszniewski L[f], Chanson M[a]

*[a]Laboratory of Clinical Investigation III, Geneva University Hospitals and University of Geneva, Switzerland, [b]Mahidol University, Bangkok, Thailand, [c]INSERM UMR 1064, CHU Nantes, ITUN, Nantes, France, [d]Department of Pathology and Immunology, Department of Internal Medicine – Cardiology, University of Geneva, Switzerland, [e]Division of Otho-Rhino-Laryngology, Geneva University Hospitals, Geneva, Switzerland and [e]Epithelix Sàrl, Plan-les-Ouates, Switzerland*

**Running title:** Human airway epithelial cell repair

**Corresponding author:**

Marc Chanson PhD

Laboratory of Clinical Investigation III

Foundation for Medical Research

64 Avenue de la Roseraie

1205 Geneva 4

Tel. +41 22 37 24 611

Fax. +41 22 34 75 979

Email: marc.chanson@hcuge.ch

## Abstract

The recovery of an intact epithelium following injury is critical for restoration of lung homeostasis, a process that may be altered in cystic fibrosis (CF). In response to injury, progenitor cells in the undamaged areas migrate, proliferate and re-differentiate to regenerate an intact airway epithelium. The mechanisms regulating this regenerative response are, however, not well understood. In a model of circular wound injury of well-differentiated human airway epithelial cell (HAEC) cultures, we identified the gap junction protein Cx26 as an important regulator of cell proliferation. We report that induction of Cx26 in repairing HAECs is associated with cell proliferation. We also show that Cx26 is expressed in a population of CK14-positive basal-like cells. Cx26 silencing in immortalized cell lines using siRNA and in primary HAECs using lentiviral-transduced shRNA enhanced Ki67-labeling index and Ki67 mRNA, indicating that Cx26 acts a negative regulator of HAEC proliferation. Cx26 silencing also markedly decreased the transcription of KLF4 in immortalized HAECs. We further show that CF HAECs exhibited deregulated expression of KLF4, Ki67 and Cx26 as well enhanced rate of wound closure in the early response to injury. These results point to an altered repair process of CF HAECs characterized by rapid but desynchronized initiation of HAEC activation and proliferation.

**Key words:** gap junctions, Cx26, cystic fibrosis, proliferation, repair, Mucilair

# 1. Introduction

The maintenance of the airway epithelium barrier integrity is required to protect lungs from environmental threats. In human, the pseudostratified airway epithelium is composed of three major cell types, including tall ciliated (CCs), mucus secreting (SCs) and basal (BCs) cells. Compared with other epithelial organs, such as the epidermis and small intestine, the airway epithelium turnover is relatively slow. However, the loss of these cells due to infection, inflammation or injury must be replaced, a process that requires the migration and proliferation of local progenitor cells, which gives rise after re-differentiation to all cell types constituting the airway epithelium (Wansleeben et al., 2013). Disruption of the coordination between proliferation and differentiation during this repair process contributes to pathological remodeling of the airway epithelium, as it is commonly observed in respiratory diseases, including cystic fibrosis (CF) (Randell, 2006; Beers, Morrissey, 2011).

Important progress has been made to detect progenitor cells and the underlying mechanisms regulating their fate in the lung (Wansleeben et al., 2013). There is evidence for stem cell niches throughout the airway tree and their capacity to regenerate normal structures has been demonstrated *in vitro* and *in vivo* (Borthwick et al., 2001; Hackett et al., 2008; Rock et al., 2009; McQualter, Bertoncello, 2012). Lineage tracing in mice during development, and in adults after injury, suggests that BCs function as long-term stem cells of the airways (Wansleeben et al., 2013). After activation, BCs self-renew and are capable of regenerating CCs and SCs. Typical markers of BCs are the transcription factor Trp63 (or p63), cytokeratin (CK)5 and CK14. On the other hand, CK8 is a marker of well-differentiated CCs and SCs that is also detected in early progenitors of these cell lineages during repair (Beers, Morrissey, 2011; Rock et al., 2011; Wansleeben et al., 2013). The mechanisms synchronizing proliferation and differentiation of activated BCs within the repairing human airway epithelium remain, however, poorly known.

Specialized cell junctions are particularly important in cellular functions essential for sustaining epithelia homeostasis. Direct cell-to-cell communication via gap junctions provides a low resistance pathway to coordinate multicellular activity via the intercellular diffusion of ions, second messengers and small metabolites (Laird, 2010). Gap junctions are formed by hexameric connexins (Cxs) at the plasma membrane, which are members of a large family of homologous proteins in vertebrates. The pattern of Cx expression by the human respiratory epithelium depends on the stage of differentiation (Chanson, Koval, 2013). For instance, Cx26 expression is elevated during the highly proliferative canalicular phase of development but is decreased with airway differentiation in ferret, mouse and human (Carson et al., 1998a). Similarly, Cx26 expression disappears from primary cultures of human airway epithelial cells (HAECs) grown at the air-liquid interface, a process associated with decreased proliferation of HAECs and differentiation to a well-polarized ciliated epithelium (Wiszniewski et al., 2007). No studies have yet investigated the expression of Cx26 during the repair process after injury of the human airway epithelium.

The skin exhibits some analogy with the lung regarding Cx26 expression. Cx26 is expressed in proliferative epidermis during early embryonic development but inhibited at terminal differentiation (Goliger, Paul, 1994; Choudhry et al., 1997). Moreover, mice lacking the Krüppel-like transcription factor 4 gene (*klf4*), which is known to act as an anti-proliferative gene (McConnel, Yang, 2010), showed severe defects in epidermal barrier acquisition with keratinocyte hyperproliferation and lesions characteristic of psoriasis (Segre Bauer, Fuchs, 1999; Djalilian et al., 2006). Interestingly, KLF4 was found to bind directly to the Cx26 promoter and repress its transcription, suggesting that enhanced keratinocyte proliferation in *Klf4*$^{-/-}$ mice is linked to Cx26 expression (Djalilian et al., 2006). Few studies have investigated KLF4 in the respiratory system and the information available has been obtained in developmental and morphogenesis studies (Wani, Wert, Lingrel, 1999; Cowan et

al., 2010). Here, we sought to determine whether Cx26 contributes to proliferation of repairing HAECs in a model of mechanical injury of well-differentiated airway epithelium in primary culture. We also evaluated whether KLF4 regulates Cx26 expression in repairing HAECs. Because a hyperproliferative state has been described in CF HAECs (Voynow et al., 2005; Hajj et al., 2007), we investigated the expression of Cx26 and KLF4 in this disease as well.

## 2. Methods and Materials

More detailed information can be found in the online supplement.

### 2.1 Airway cell cultures

HAECs cultured at the air-liquid interface were prepared as previously described (Wiszniewski et al., 2006). Materials were obtained from patients undergoing surgical endonasal polypectomy or partial middle turbinectomy. Briefly, HAECs obtained by protease digestion of airway biopsies were grown in CnT-17 medium (CELLnTEC, Bern, Switzerland) supplemented with 30 U/ml penicillin and 30 mg/ml streptomycin on flasks coated with PureCol (Advanced BioMatrix, San Diego, CA) until a monolayer was established. HAECs were then isolated, seeded on Transwell inserts and allowed to differentiate at the air-liquid interface for 30-60 day. The basal medium, which consisted of DMEM:F12 (3:1) supplemented with 1.5% Ultroser G (Life Sciences, Zug, Switzerland) and antibiotics, was refreshed every 2 days. For experiments comparing control (Ctrl) and CF epithelia, polarized HAEC cultures (MucilAir$^{TM}$ and MucilAir$^{TM}$-CF) were provided by Epithelix (Sàrl Epithelix Sàrl, Plan-Les-Ouates, Switzerland). All CF HAEC cultures were generated from patients homozygous for the F508del mutation except 1 patient heterozygous for the F508del mutation and an unknown mutation.

UNCN1T, UNCN2T and UNCN3T human bronchial epithelial cell lines were maintained in the CnT-17 medium supplemented with antibiotics (Fulcher et al., 2009).

### 2.2 RNA Silencing and ReverseTranscription Polymerase Chain Reaction

UNCN cells were transfected with small interfering RNA (siRNA) specific for Cx26, KLF2 and KLF4 using Steath RNAi$^{TM}$ siRNAs (Invitrogen, Lucerne, Switzerland). The Stealth

RNAi$^{TM}$ siRNA negative controls that do not target (siNT) any known human sequence were used to test for specificity of the silencing strategy.

Primary HAECs were transduced with lentiviral vectors expressing a short hairpin RNA (shRNA) directed against Cx26 or a scramble sequence (shAlter). A GFP reporter gene expression cassette driven by the elongation factor 1 alpha promoter was also contained in the vectors. HAECs seeded on Primaria Petri dishes (Becton Dickinson, Meylan, France) at low density were transduced with lentiviral vectors at an MOI of 10 in CnT-17 medium containing 2 µg/mL polybrene (Sigma). After three days, GFP positive cells were FACS and immediately analyzed for mRNA expression.

Total cellular RNA was isolated from UNCN cells or HAECs and reversed transcribed for qPCR. The thermal cycle (CT) of each gene was detected and subtracted from the CT of 18S to obtain ΔCT to calculate $2^{-2\Delta CT}$ or $2^{-\Delta\Delta CT}$ (fold increase).

**2.3 Wound closure assay**

Reproducible circular wounds were made on well-differentiated HAEC cultures by using an airbrush linked to a pressure regulator. Data were expressed as % of wound closure, 100% representing complete wound closure.

**2.4 Western Blotting and Immunohistochemistry**

Western blots and immunofluorescence staining were performed as previously described (Wiszniewski et al., 2007). Immunostaining was performed on UNCN and HAEC cells or frozen sections of human polyps after fixation with 4% paraformaldehyde for 15 min, and on sections of paraffin-embedded HAEC cultures after 1h-24h fixation.

**2.5 Statistical Analysis**

GraphPad Prism software (version 4.03) was used to compare experiments with paired or unpaired *t*-tests, where appropriate. Values are expressed as Mean ± SEM. $P<0.05$ (*) was considered significant.

## 3. Results

### *3.1 HAEC repair involves transient proliferation*

Primary cultures of HAECs grown at the air-liquid interface for at least 30 days were used. In this model, HAECs reproduced the 3D structure of well-differentiated, non-proliferating, airway epitheliums with BCs, SCs and CCs in a context devoid of exogenous infection or inflammation (Wiszniewski et al., 2006). To induce BC activation, a circular wound was mechanically made and repair was monitored as a function of time. As shown in Fig. 1a, two areas were defined: HAECs at the periphery of the wound (back) and repairing cells that progressively cover the denuded region (front) with time (top right panel). The undamaged HAECs at the back of the wound therefore represent the population of cells that initiate the repair process. Histology of the transition between back and front areas shows the decrease in height of the repairing epithelium (Fig. 1b). The kinetic of wound healing was evaluated from time-lapse microscopy and expressed as percentage of wound repair (Fig. 1c). The wounded area was covered by 50% within 24h and wound healing was completed after 48h in 6 out of 7 HAEC cultures. The wound healing rate, which for a concentric injury could be reliably measured at early time points of repair, gave a mean ± SEM value of 0.16 ± 0.03 $mm^2$/h (n=7) and of 0.19 ± 0.02 $mm^2$/h (n=7) during the 12h and 24h post-wounding, respectively.

HAEC proliferation in response to injury was monitored by immunostaining of the nuclear proliferation marker Ki67. Ki67 expression was detected at the wound edge already 12h after wounding and peaked over a period ranging between 48 and 60h, around the time of wound closure (Fig. 1d). The number of Ki67-positive cells decreased dramatically at later times after complete closure of the wound (Fig. 1d). Cell proliferation, measured at the back and front areas, was quantified by determining the Ki67-labeling index on HAEC cultures from 4 different donors (Fig. 1e). Although variable between primary cultures from different

donors, a strong increase of the Ki67-labeling index at the front area of repairing cells but not in the undamaged cells at the back area was observed (Fig 1e).

These results indicate that well-differentiated HAECs can initiate wound repair in response to injury via a process that involved migration and induction of proliferation. Proliferation ceased, however, after completion of wound closure.

### *3.2 Cx26 expression is induced in repairing HAECs*

The human airway epithelium expresses different types of gap junction proteins; however, Cx26 was not detectable in well-differentiated primary HAEC cultures (Wiszniewski et al., 2007). Upon wounding, we observed that Cx26 expression is induced in repairing HAECs; at 12h post-wounding, intracellular and some junctional staining could be observed while Cx26 localized only at cell-cell contacts 48h after injury (Fig. 2a). Quantitative PCR showed a 2-fold increase ($P<0.04$) in Cx26 mRNA within 12h post-wounding, a level that was maintained in repairing cells up to 48h (Fig. 2b). Quantification of the immunofluorescence signal in cultures from 5 donors showed changes in Cx26 signal with a time course that closely resembles the one of Ki67. Cx26 is detectable 12h after wounding at the edge of the wound and its expression markedly increased with time to peak at a 48-60h after injury in the front area (Fig. 2c). Like Ki67, Cx26 was transiently detected in repairing HAECs, the expression of the protein decreasing from 60h on after complete closure of the wound (Fig. 2c).

To examine the relationship between Ki67 and Cx26, we performed co-immunostainings in repairing HAECs. As shown in Supplemental Fig. 1a, this approach revealed complex patterns of expression with immunodetection of clusters of cells positive only for Cx26 or for Ki67, as well as clusters of cells positive for both Cx26 and Ki67. The expression of Cx26 in Ki67-negative and Ki67-positive cells was confirmed by confocal microscopy (Supplemental Fig. 1b). This complex and heterogeneous pattern of Cx26 and

Ki67 expression within the repairing area was observed at all time points after wounding. Both cell migration and proliferation contribute to the spatiotemporal dynamic of the wound healing process. In order to evaluate the relative contribution of these processes on Cx26 expression, we have treated HAEC cultures wounded for 48h, the time at which Cx26 is maximally induced, with Y27632 or mitomycine C (Fig. 2d). Y27632 is a widely used inhibitor of cell migration by blocking RhoA-dependent reorganization of the F-actin cytoskeleton. Interestingly, the detection of both Cx26 and Ki67 was increased in response to the cell migration inhibitor. In contrast, the expression of both Cx26 and Ki67 was virtually abolished in the presence of mitomycine C, an inhibitor of cell division. These results suggest that cell division is required to trigger the expression of Cx26 in repairing HAECs

Repairing HAECs enter a program of proliferation and re-differentiation that can be followed by the expression of specific cell markers (Wansleeben et al., 2013). As shown in Fig3a, The typical expression pattern of these markers was recapitulated in primary HAEC cultures with the detection of CK5 and CK14 in BCs, and of CK8 in CCs. We next evaluated for their expression in repairing HAECs 24h after wounding, an early time point at which the expression of Cx26 is markedly induced. As shown in Fig. 3a (top right panel), the first layer of cells covering the denuded area was made of CK5-positive cells. We also performed co-immunostaining for Cx26 and CK8. As shown on a gallery of confocal microscope images in Fig. 3b, the expression of Cx26 was restricted to the basal layer of HAECs in the front area. CK8-expressing cells were located in the superior layer of repairing HAECs. Finally, and consistent with its basal localization, we found that Cx26 was expressed in a population of HAECs positive for CK14 (Fig. 3c).

These results indicate that in repairing HAECs, Cx26 expression is detected at the front area of the wound in BCs positive for CK14.

### *3.3 Cx26 modulate airway epithelial cell proliferation*

To further study the relationship between Cx26 and cell proliferation, we searched for human airway epithelial cell lines expressing this gap junction protein. Recently, HAECs from three donors have been immortalized by introduction of Bmi-1 and the catalytic subunit of telomerase (hTERT) into primary bronchial cells (Fulcher et al., 2009). These three Bmi-1/hTERT airway epithelial cell lines (UNCN1T, UNCN2T and UNCN3T; globally referred to as UNCN cells) express high levels of Cx26 at cell-cell contacts as revealed by immunostaining and Western blot (Supplemental Fig. 2a and b). We next developed a silencing strategy using siRNAs to reduce functional expression of Cx26 in these cell lines. Three different siRNAs and a mixture of them (siRNAMix) were tested on all three UNCN cell lines. As shown in Supplemental Fig. 2c, we found that siRNA2 and siRNAMix (hereafter referred to as siCx26) were the most efficient ($P<0.01$). Next, we evaluated the effects of siCx26 on the Ki67-labeling index of UNCN cells. We observed that siCx26 increased ($P<0.05$) proliferation of UNCN cells as compared to cells transfected with a non targeting control siRNA (siNT; Fig. 4a).

In skin, KLF4 represses the expression of Cx26 and exerts anti-proliferative effects (McConnel, Yang, 2010). To investigate whether KLF4 is also involved in the regulation of Cx26 and proliferation in airway epithelial cells, we performed RT-qPCR on mRNAs isolated from UNCN1T and UNCN2T cells transfected with siCx26 or a siRNA against KLF4 (siKLF4). Surprisingly, siKLF4 had no effect on Cx26 mRNA levels in these cells (Fig. 4b). In contrast, we found that silencing Cx26 decreased mRNA levels of KLF4 (Fig. 4c). We also evaluated the effect of silencing of KLF2, a typical lung Krüppel-like Factor with high expression in this organ (Wani, Wert, Lingrel, 1999). KLF2 silencing had no effect of Cx26 expression nor did Cx26 silencing affect KLF2 expression in UNCN1T and UNCN2T cells

(Fig. 4b and d). Of note, the efficiency of each siRNA (siCx26, siKLF4 and siKLF2) was verified and confirmed at the mRNA level in each experiment (Fig.4b, c and d).

Gene silencing of basal cells in well-differentiated HAEC cultures could not be achieved. To confirm the anti-proliferative effect of Cx26, non-differentiated HAECs obtained from 4 patients were cultured on Petri dishes and transduced by lentiviral vectors co-expressing green fluorescent protein (GFP) and specific shRNA sequences targeting the mRNAs of Cx26 (shCx26) or a control shRNA (shAlter). Cx26 and Ki67 mRNA levels were determined by RT-qPCR in transduced HAECs expressing GFP. Relative to shAlter, shC26 efficiently decreased Cx26 mRNA by 77% (0.23 ± 0.06, n=4; $P<0.01$). In 3 out 4 experiments, an increased of Ki67 mRNA (1.8 ± 0.3; $P<0.05$) was observed. In contrast, shCx26 did not affect (1.1 ± 0.2, n=4) KLF4 mRNA. However, it is important to note that in non-differentiated HAECs, the mRNA level of this gene was extremely low ($2^{-\Delta CT}$: 2.8 $10^{-5}$ ± 4 $10^{-6}$, n=4).

All together, these results indicate that Cx26 negatively regulates cell proliferation and suggest that transcription of Cx26 in HAECs is not dependent on KLF4 or KLF2.

### *3.4 Cx26 expression, KLF4 transcription and proliferation in repairing CF HAECs*

As abnormal epithelial repair is a hallmark of CF (Randell, 2006; Beers and Morrissey, 2011), we therefore investigated Cx26 and KLF4 expression as well as proliferation in HAECs obtained from CF patients. We have first verified the expression levels of Cx26 and KLF4 in well-differentiated primary cultures of CF HAECs by RT-qPCR. As shown in Fig. 5a, Cx26 and KLF4 expression was similar in control and CF HAECs; KLF4 mRNA level was 10 times higher as compared to non-differentiated HAECs. We then monitored the expression of KLF4 in repairing HAECs following injury. As shown in Fig. 5b, the relative changes of KLF4 mRNA to the non-injured conditions (0h) showed a transient increase during the early

time points after injury in control cultures. KLF4 mRNA increased rapidly following airway epithelium injury and progressively decreased down to initial values. Importantly, this transient modulation in KLF4 mRNA transcription was not observed in CF HAECs; the mRNA levels for KLF remained unchanged during wound repair (Fig. 5c). We have also monitored the time course of KLF2 mRNA level during repair of control and CF HAECs. Again, like KLF4, the transient induction of KLF2 mRNA at 12h post-wounding was not observed in CF HAECs (Fig. 5b).

The Ki67-labeling index was then determined at front and back areas of repairing CF HAECs during wound repair. Similar to control cultures, the Ki67-labeling index increased after wounding in the front area at 12h and remained elevated for up to 60h post-wounding before decreasing progressively at later time points (Fig. 6a). In contrast with control HAECs that showed no proliferation in the back area (Fig. 1e), Ki67-positive cells were readily detected in the back area of repairing CF HAEC cultures at all time points. Representative examples of Ki67 detection during repair in Ctrl HAECs and CF HAECs are shown in Supplemental Fig. 3. Indeed, the Ki67 signal is present in an organized concentric manner around the wound edge but restricted to the front area in all Ctrl HAECs, whereas a heterogeneous disorganized signal is detected in repairing CF HAECs from 3 out of 4 donors. Cx26 expression was also detected in the back area in CF HAECs undergoing repair, as quantified in Fig. 6b. Finally, we measured the time course of wound closure in CF HAEC cultures (Fig. 6c). CF HAECs showed a faster kinetic ($P<0.05$) of wound closure at 12h and 24h post-injury as compared to control HAECs (Fig. 6c). The rate of wound healing was 0.23 ± 0.02 $mm^2/h$ (n=5; $P<0.05$) during the first 12 hours of repair in CF HAECs. No significant differences in wound healing rates between control and CF HAECs were, however, observed for later time points. The early difference may be explained by a different composition of control and CF cell population obtained from donors to generate the primary cultures. In fact,

HAECs obtained from CF patients may exhibit enhanced amount of activated stem cells in response to chronic inflammation and infection. To evaluate this hypothesis, we quantified by RT-qPCR the expression levels of Sox2, a marker of airway epithelial cell differentiation (Fig. 6d), as well as of unique stem cell markers (Nanog and OCT3/4) in Ctrl and CF HAEC cultures before wounding (Fig. 6e and f). Comparable expression levels of Sox2, Nanog and OCT3/4 mRNAs were however observed in Ctrl and CF HAEC cultures.

Collectively, these results indicate that the transcription factors KLF4 and KLF2 are rapidly induced following epithelial injury in Ctrl HAECs undergoing repair. This rapid induction is lost in CF HAECs.

## 4. Discussion

The mechanisms regulating the maintenance of the human pseudostratified airway epithelium are poorly known. In this study, we evaluated the wound repair process of well-differentiated HAEC cultures. We report that upon injury, expression of the gap junction protein Cx26 is transiently induced in a population of basal-like cells, a phenomenon associated with ceased proliferation of HAECs. We further show that in response to injury, CF HAECs exhibit altered coordination of Cx26 expression and proliferation as well as an enhanced rate of wound healing at the early phase of the repair process. Finally, the early and transient induction of KLF4, a transcription factor known to negatively regulate cell proliferation, was absent in CF HAECs undergoing repair.

It is well established that gap junctions contribute to cell homeostasis by allowing the intercellular exchange of essential growth regulators, including ions, nucleotides, sugars, small peptides, RNAs (Kardamia et al., 2007; Vinken et al., 2011), and microRNAs (Lim et al., 2011). Cx26 expression is virtually absent in the normal adult airway epithelium (Chanson, Koval, 2013). We observed that its expression is induced in HAECs undergoing wound repair. Proliferation and Cx26 expression were transiently increased following injury but both events terminated after wound closure was completed. Furthermore, Cx26 expression was induced by proliferation but abolished by inhibitors of cell division. One interpretation of these results is that the expression of Cx26 is triggered in daughter cells of an expanding, but not yet differentiating, population of BCs, in response to proliferative signals generated by the injured epithelium. Cx26 was not detected in CK8-positive cells, which represent early progenitors of SC and CC lineages (Rock et al., 2011), but is present in a population of CK14-positive HAECs. An early report in the rat tracheal epithelium and later mouse genetic-lineage tracing studies showed that the proportion of CK14-expressing BCs transiently increased following epithelial damage, suggesting that CK14 is up-regulated when BCs are

activated (Hong et al., 2004; Ghosh et al., 2010). Thus, our results suggest that Cx26 expression is induced in BCs activated for proliferation during the repair process; Cx26 expression, however, is strongly repressed with differentiation. This interpretation is consistent with recent studies showing that a transient population of CK5/CK14-positive basal like cells is capable of self-renewal and can regenerate SCs and CCs (Rock et al., 2009; Kumar et al., 2011).

Cx26 exerts an anti-proliferative role as evaluated by determining the Ki67-labeling index and Ki67 mRNA. Interestingly, Cx26 could be observed at the junctional membrane of Ki67-positive cells, Ki67-negative cells and between Ki67-positive and Ki67-negative cells. This observation suggests that Cx26 is present in different populations of HAECs (Ki67-negative and Ki67-positive) or that co-expression of both proteins in one cell population is transient. Given that one dividing BC can give rise to two daughters BCs, or one BC and one early progenitor cell (EP) or two EPs, and that these processes of symmetric and asymmetric division behave in a stochastic manner (Teixeira et al. 2013), it was impossible to detect the sequential expression of these two proteins as a function of time of repair in a 3D culture model of primary HAECs.

There is a body of evidence implicating gap junctions as growth suppressors in several tissues but a direct connection between the exchange of signaling molecules between cells through gap junctions and the control of cell proliferation has not been established (Kardami et al., 2007). Using sophisticated techniques, it was recently reported that Cx26 redistributes cAMP between cancer cells that, in turn, blocks cell division (Chandrasekhar et al., 2013). Such a mechanism may also explain how exogenous expression of Cx26 improved barrier function and maintained tight junctions in Calu-3 airway epithelial cells (Go et al., 2006). Indeed, Cx26 expression may decrease proliferation in this cell line, thus favoring cell-cell contacts and the establishment of a tight epithelium. In this context, the tight junction

associated protein occludin was shown to bind Cx26 via coiled-coil domain interaction (Nusrat et al., 2000). Thus, induction of Cx26-mediated intercellular communication by proliferative signals in repairing BCs may represent a mean to repress their proliferation and progressively promote the formation of a tight monolayer, which may serve as a platform for later differentiation. The signaling factors that regulate the on/off expression of Cx26 during the repair process remained to be identified.

An inverse relationship between KLF4 and Cx26 expression has been observed in keratinocytes from *klf4*-deficient mice. It was suggested that persistent expression of Cx26 in suprabasal cells, by virtue of the involucrin promoter, maintained the epidermis in a hyper-proliferative state (Djalilian et al., 2006), suggesting that Cx26 stimulated proliferation. This scenario was not supported in a recent study reporting that ectopic expression of Cx26 in basal keratinocytes using the CK5 promoter showed a tendency to decrease proliferation but had no pathological skin alteration as compared to control mice (Wang et al., 2010). We found in HAECs that silencing Cx26 markedly decreased mRNA levels of KLF4 while down-regulation of KLF4 had no effects on Cx26 mRNA. Thus, induction of Cx26 in repairing HAECs is likely the consequence of increased proliferation rather than inhibition of transcriptional repression by KLF4. KLF4 levels are generally elevated in differentiated tissues as compared to proliferating and cancer cells (McConnel, Yang, 2010). As expected, KLF4 mRNA was 10 times lower in proliferating HAECs as compared to well-differentiated cultures. Therefore, it cannot be ruled out that the decreased KLF4 transcription observed during Cx26 gene silencing is an indirect consequence of enhanced proliferation.

Cx26 and KLF4 are both key factors in the balance between proliferation and differentiation and we hypothesized that alteration in this coordinated process may result in abnormal repair and remodeling of HAECs, as observed in many respiratory diseases. We have found that the transcriptional activity of *klf2* and *klf4* genes is induced transiently in

response to wounding, a phenomenon that was absent in CF HAECs. In CF cultures, however, we observed prompt induction of proliferation and of Cx26 expression at the early phases of wound repair, as well as enhanced initial rate of wound closure as compared to Ctrl HAECs. These results may relate to the hyper-proliferative state previously described in CF HAECs (Voynow et al., 2005; Hajj et al., 2007). The rapid onset of proliferation in CF HAECs could be explained, in part, by increased amount of progenitor cells in these cultures. This did not appear to be the case since no difference was detected in mRNAs of KLF4, Nanog, and OCT3/4 between control and CF HAECs. Thus, our results suggest that the balance between pro-and anti-proliferative signals is altered in repairing CF HAECs.

Recent data have reported the critical role of the cystic fibrosis transmembrane conductance regulator (*Cftr*) gene in airway epithelial wound healing (Schiller et al., 2010; Trinh et al., 2012). Although the mechanisms connecting *Cftr* deficiency to defective *klf4* induction and enhanced HAEC activation remain to be established, our results point to a disturbed repair process of CF HAECs characterized by fast but desynchronized initiation of BC activation and proliferation in a primary 3D model of epithelium damage.

## Acknowledgements

This work was supported by the Swiss National Science Foundation (grants 310000–119739 and 310030_134907/1) to M.C. S.C was supported by “Vaincre la Mucoviscidose”, “Téléthon Action Suisse” and “Novartis Stiftung für Medizinisch Biologische Forschung”. We are indebted to Dr. SH Randell (Cystic Fibrosis/Pulmonary Research and Treatment Center, The University of North Carolina at Chapel Hill, Chapel Hill, NC, USA) for providing us with the UNCN airway cell lines. We thank Isabelle Scerri and Davide Losa for technical help and discussion during the progression of this project.

## References

Beers MF, Morrissey EE. The three R's of lung health and disease: repair, remodelling, and regeneration. J Clin Invest 2011;121:2065-2073.

Borthwick DW, Shahbazian M, Krantz QT, et al. Evidence for stem-cell niches in the tracheal epithelium. Am J Respir Cell Mol Biol 2001;24:662-670.

Carson JL, Reed W, Moats-Staats BM, et al. Connexin26 expression in human and ferret airways and lung during development. Am J Respir Cell Mol Biol 1998;18:111-119.

Chandrasekhar A, Kalmykov EA, Srikanth R, et al. Intercellular redistribution of cAMP underlies selective suppression of cancer cell growth by Connexin26. PLoS One 2013; 8:e82335.

Chanson M, Koval M. Connexins in lung function and inflammation. In: Connexin Cell Communication Channels: Roles in the Immune System & Immunopathology / ed. E. Oviedo-Orta, B.R. Kwak, WH Evans – CRC Press (2013) – pp. 137-156.

Cowan CE, Kohler EE, Dugan TA, et al. Kruppel-like factor-4 transcriptionally regulates VE-cadherin expression and endothelial barrier function. Circ Res 107;959-66, 2010.

Djalilian AR, McGaughey D, Patel S, et al. Connexin26 regulates epidermal barrier and wound remodelling and promotes psoriasiform response. J Clin Invest 2006;116:1243-1253.

Fulcher ML, Gabriel SE, Olsen JC, et al. Novel human bronchial epithelial cell lines for cystic fibrosis research. Am J Physiol Lung Cell Mol Physiol 2009;296:L82-L91.

Go M, Kojima T, Takano K, et al. Connexin 26 expression prevents down-regulation of barrier and fence functions of tight junctions by Na+/K+-ATPase inhibitor ouabain in human airway epithelial cell line Calu-3. Exp Cell Res 2006;312:3847-3856.

Ghosh M, Brechbuhl HM, Smith RW, et al., Context-dependent differentiation of multipotential keratin14-expressing tracheal basal cells. Am J Respir Cell Mol Biol 2010;45:403-410

Hackett T-L, Shaheen F, Johnson A, et al. Characterization of side population cells from human airway epithelium. Stem cells 2008;26:2576-2585.

Hajj R, Lesimple P, Nawrocki-Raby B, et al. Human airway surface epithelial regeneration is delayed and abnormal in cystic fibrosis. J Pathol 2007;211:340-350.

Hong KU, Reynolds SD, Watkins S, et al. In vivo differentiation potential of tracheal basal cells: evidence for multipotent and unipotent subpopulations. Am J Physiol Cell Mol Physiol 2004;286:L643-L649.

Kardamia E, Danga X, Iacobasb DA, et al. The role of connexins in controlling cell growth and gene expression. Progress in Biophysics and Molecular Biology 2007;94:245–264.

Kumar PA, Hu Y, Yamamoto Y, et al. Distal airway stem cells yield alveoli in vitro and during lung regeneration following H1N1 influenza infection. Cell 2011:147:525-538.

Laird DW. The gap junction proteome and its relationship to disease. Trends Cell Biol 2010;20:92-101.

Lim PK, Bliss SA, Patel SA, et al. Gap junction-mediated import of microRNA from bone marrow stromal cells can eleicit cell cycle quiescence in breast cancer cells. Cancer Res 2011;71:1550-1560.

McConnell BB, Yang VW. Mammalian Krüppel-Like Factors in Health and Diseases. Physiol Rev 2010;90:1337–1381.

McQualter JL, Bertoncello I. Concise Review: Deconstructing The Lung To Reveal Its Regenerative Potential Stem Cells. Stem Cells 2012. doi: 10.1002/stem.1055.

Nursat A, Chen JA, Foley CS, et al. The coiled-coil domain of occludin cana ct to organize structural and functional elements of the epithelial tight junction. J Biol Chem 2000; 275:29816-29822.

Randell SH. Airway epithelial stem cells and the pathophysiology of chronic obstructive pulmonary disease. Proc Am Thorac Soc 2006;3:718–725.

Rock JR, Gao X, Xue Y, et al. Notch-dependent differentiation of adult airway basal stem cells. Cell Stem Cell 2011;8 :639-648.

Rock JR, Onaitis MW, Rawlins EL, et al. Basal cells as stem cells of the mouse trachea and human airway epithelium. Proc Natl Acad Sci U S A 2009;106:12771-12775.

Segre J-A, Bauer C, Fuchs E. Klf4 is a transcription factor required for establishing the barrier function of the skin. Nat Genet 1999;22:356-360.

Schiller KR, Maniak PJ, O'Grady SM. Cystic fibrosis transmembrane conductance regulator is involved in airway epithelial wound repair. Am J Physiol Cell Physiol 2010;299:C912-21.

Teixeira VH, Nadarajan P, Graham TA, et al. Stochastic homeostasis in human airway epithelium is achieved by neutral competition of basal cell progenitors. eLife 2013;2:e00966.

Trinh NT, Bardou O, Privé A, et al. Improvement of defective cystic fibrosis airway epithelial wound repair after CFTR rescue. Eur Respir J 2012;40:1390-400.

Vinken M, Decrock E, De Vuyst E, et al. Connexins: sensors and regulators of cell cycling. Biochim Biophys Acta 2011;1815:13-25.

Voynow JA, Fischer BM, Roberts BC, Proia AD. Basal-like cells constitute the proliferating cell population in cystic fibrosis airways. Am J Respir Crit Care Med 2005;172:1013-1018.

Wang X, Ramurez A, Budunova I. Overexpression of Connexin26 in the basal keratinocytes reduces sensitivity to tumor promoter TPA. Exp Dermatology 2010;19:633-640.

Wani MA, Wert SE, Lingrel JB. Lung Kruppel-like factor, a zinc finger transcription factor, is essential for normal lung development. J Biol Chem 1999;274 :21180–21185.

Wansleeben C, Barkauskas CE, Rock JR, Hogan BLM. Stem Cells of the adult lung: their development and role in homeostasis, regeneration and disease. WIREs Dev Biol 2013;2:131-148.

Wiszniewski L, Jornot L, Dudez T, et al. Long-term cultures of polarized airway epithelial cells from CF patients. Am J Respir Cell Mol Biol 2006;34:39-48.

Wiszniewski L, Sanz J, Scerri I, et al. Functional expression of connexin30 and connexin31 in the polarized human airway epithelium. Differentiation 2007;75:382-392.

## Figure legends

**Figure 1:** Proliferation is induced in response to wounding of a 3D model of HAECs in primary cultures. **a)** HAECS were cultured at the air-liquid interface on Transwell porous filters undercoated with a feeder layer of human fibroblasts. Representative images of a well differentiated culture taken at subsequent times post-wounding are shown (top left panels). This allowed delineating the undamaged area (back) by the wound and the repairing area (front) of HAECs that progressively covered the denuded area (top right panel). Note that wound was closed 48h after injury in this experiment. **b)** A paraffin section made in a culture 48h after wounding to illustrate the histology of HAECs undergoing repair. Bar=200 μm. **c)** Time course of wound closure measured in Ctrl HAECs (n=7) undergoing repair after wounding. **d)** Representative images of Ki67 immunostaining (red) on HAECs cultures 12, 24, 36, 48, 60, 72 and 96 hours post-wounding. The dotted line in images at 12h and 24h post-wounding delineates the denuded area. Bar=100 μm. **e)** The Ki67-labeling index (%) was determined in the front and back areas of HAECs undergoing repair at various times post-wounding. *$P$<0.05 front *vs.* back areas; n=4.

**Figure 2:** Cx26 expression in Ctrl HAECs in response to wounding. **a)** Representative confocal images of Cx26 immuno-detection in response to wounding. Typically, Cx26 (green) was observed in the front areas of repairing HAECs already 12h post-wounding. Highest levels of Cx26 expression was detected 48h post-wounding and decreased thereafter to almost basal levels after 96h of repair. Nuclei were stained with DAPI (blue). Bar=25 μm. **b**) Changes in Cx26 mRNA was monitored by RT-qPCR at different times post-wounding. Values were calculated as $2^{-\Delta CT}$, normalized to the mRNA level at time 0 and thus expressed as fold changes. *$P$<0.04 front *vs.* back areas; n=4-7. **c)** The Cx26 signal was quantified (integrated area) in the front and back areas of HAECs undergoing repair for different times

post-wounding. *$P$<0.02 front *vs.* back areas; n=5. **d)** Confocal images (with x-z projections) of co-immunostaining for Cx26 (green) and Ki67 (red) in repairing HAECs 24h post-wounding before (left panel) and after treatment with 100 μM Y27632 (middle panel) or 1 μg/ml mitomycin C (right panel). Nuclei stained with DAPI are in blue. Bar=25 μm.

**Figure 3:** Cx26 is expressed in a basal-like cell population. **a)** Immunodetection of CK5, CK14 and CK8 on HAEC primary cultures. Basal cells are positive for CK5 (red, left top panel) and CK14 (red, bottom right panel) while tall ciliated cells are positive for CK8 (green, bottom left panel; arrows show negative basal cells). After wounding, the cells that migrate out at the front edge are positive for CK5 (red, right top panel, arrow). Bar=40 μm in top panels and 25 μm in the bottom panels. **b)** Co-immunostaining for Cx26 (green) and CK8 (red) in repairing HAECs at the front area 48h after wounding. Gallery of successive confocal images (from 1 to 8, taken every 2 μm) through the height of the airway epithelium (apical to basal) is shown. Cx26 is mostly localized in basal cells (images 7 and 8) below differentiating cells expressing CK8. Bar=25 μm. **c)** Representative confocal images (corresponding to height similar to images 7 and 8 in panel b) showing the co-expression of Cx26 and CK14 in repairing HAECs for 24h. Nuclei are stained with DAPI (blue). Bar=25 μm.

**Figure 4: a)** Transfection of UNCN cells with siCx26 increased the number of proliferative cells, as detected by Ki67 immunostaining. Values are expressed as ratios to the number of Ki67 cells measured in cells treated with lipofectamine only (Lipo). The number of Ki67-positive cells in cells transfected with a control siRNA (siNT) is also shown. Values were obtained after transfection of UNCN1T (repeated 3 times), UNCN2T (repeated 4 times) and UNCN3T (1 time) with siCx26. Because no difference was observed between the three lines (UNCN1T: 2.3 ± 0.3; UNCN2T: 2.4 ± 0.8; UNCN3T: 2.45), data were pooled; $P$<0.01. **b)**

Pooled data from RT-qPCR for Cx26 mRNA obtained from UNCN1T (n=4) and UNCN2T (n=2) cells silenced with siCx26, siKLF2 or siKLF4; $P<0.01$. **c)** Pooled data from RT-qPCR for KLF2 mRNA obtained from UNCN1T (n=3) and UNCN2T (n=2) cells silenced with siCx26, siKLF2 or siKLF4; $P<0.01$. **d)** Pooled data from RT-qPCR for KLF4 mRNA obtained from UNCN1T (n=4) and UNCN2T (n=1) cells silenced with siCx26, siKLF2 or siKLF4; $P<0.01$. In **b-d**, values were calculated as $2^{-\Delta CT}$, normalized to cells treated only with lipofectamine (Lipo) and thus expressed as $2^{-\Delta CT}$ (fold changes). Relative changes in mRNA for each gene of interest in cells transfected with a control siRNA (siNT) are also shown.

**Figure 5:** Absence of KLF4 mRNA induction in response to injury of CF HAECs. **a)** RT-qPCR for Cx26 and KLF4 mRNAs obtained from control (Ctrl) and CF HAECs. Values were calculated as $2^{-\Delta CT}$; Cx26: n=9 (Ctrl HAECs) and 8 (CF HAECs), respectively. KLF4: n=8 (Ctrl HAECs) and 5 (CF HAECs), respectively. **b)** Relative changes in KLF4 (left panel) and KLF2 (right panel) mRNAs in Ctrl HAECs undergoing repair for increasing times after wounding. **c**) Relative changes in KLF4 (left panel) and KLF2 (right panel) mRNAs in CF HAECs undergoing repair for increasing times after wounding. Values were calculated as $2^{-\Delta CT}$ and normalized to values measured in non-wounded cultures (time 0). n=3-9; $P<0.05$.

**Figure 6: a)** The Ki67-labeling index (%) was determined in the front and back areas of CF HAECs undergoing repair for different times post-wounding. Of note, Ki67 detection between front and back areas was not significantly different; n=4. **b)** Quantification of the Cx26 signal (integrated area) in the front and back areas of CF HAECs undergoing repair for different times post-wounding. Again, no significant difference in Cx26 expression between front and back areas was observed. n=6. **c)** Time course of wound closure measured in CF HAECs (n=5) undergoing repair after wounding. The time course of wound closure from Ctrl HAECs

(grey line) is redrawn from Fig.1c for comparison purposes; $P<0.015$. **d)** RT-qPCR for Sox2 mRNA obtained from control (Ctrl) and CF HAECs. n=5 (Ctrl HAECs) and 3 (CF HAECs), respectively. **e)** RT-qPCR for Nanog mRNA obtained from control (Ctrl) and CF HAECs. n=9 (Ctrl HAECs) and 6 (CF HAECs), respectively. **f)** RT-qPCR for OCT3/4 mRNA obtained from control (Ctrl) and CF HAECs. n=10 (Ctrl HAECs) and 5 (CF HAECs), respectively. In **d**, **e**, **f**), values were calculated as $2^{-\Delta CT}$.

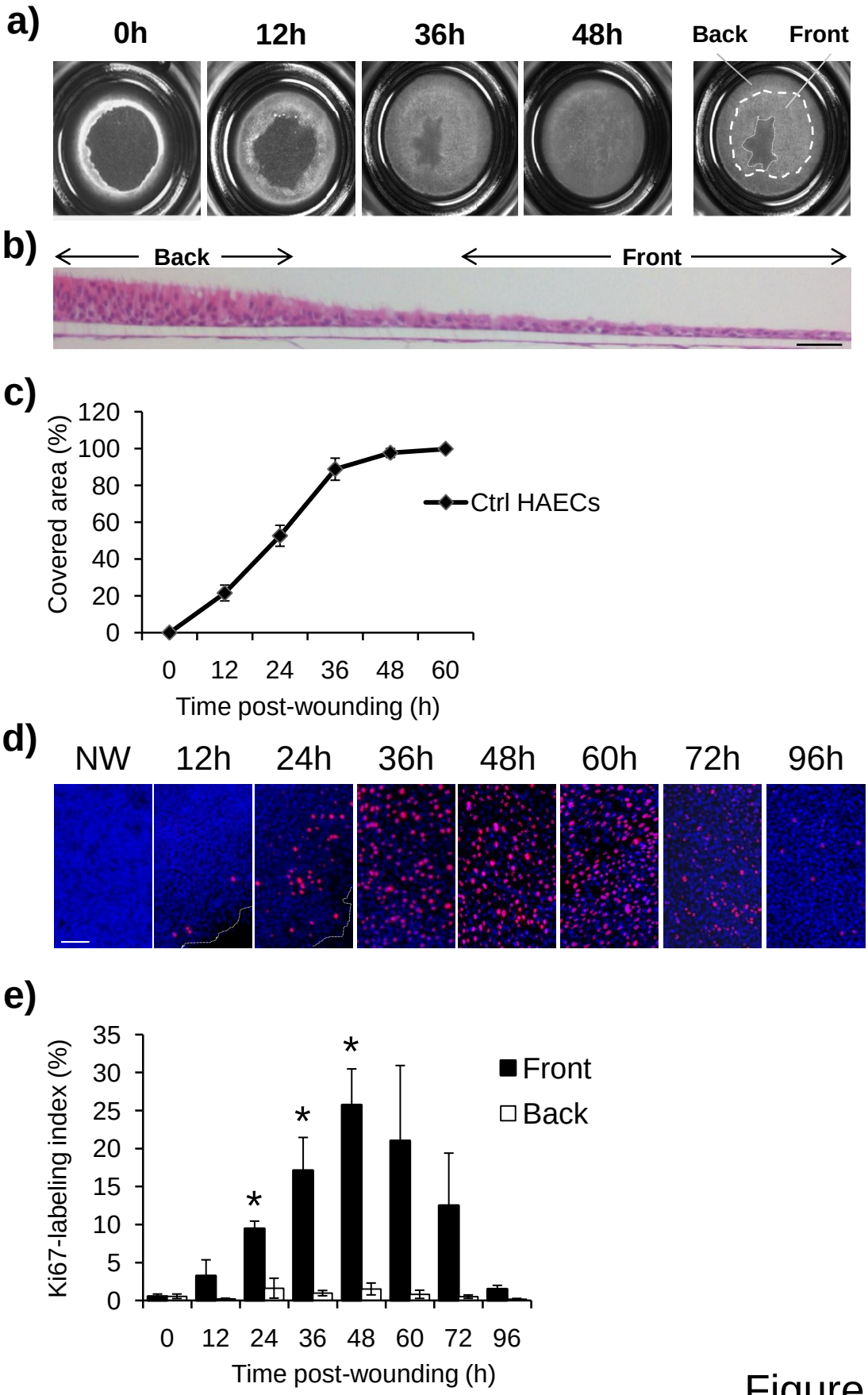
a)
0h
12h
36h
48h
Back
Front
b)
Back
Front
c)
Covered area (%)
120
100
80
60
40
20
0
0
12
24
36
48
60
Time post-wounding (h)
Ctrl HAECs
d)
NW
12h
24h
36h
48h
60h
72h
96h
e)
Ki67-labeling index (%)
35
30
25
20
15
10
5
0
*
*
*
0
12
24
36
48
60
72
96
Time post-wounding (h)
Front
Back

Figure 1

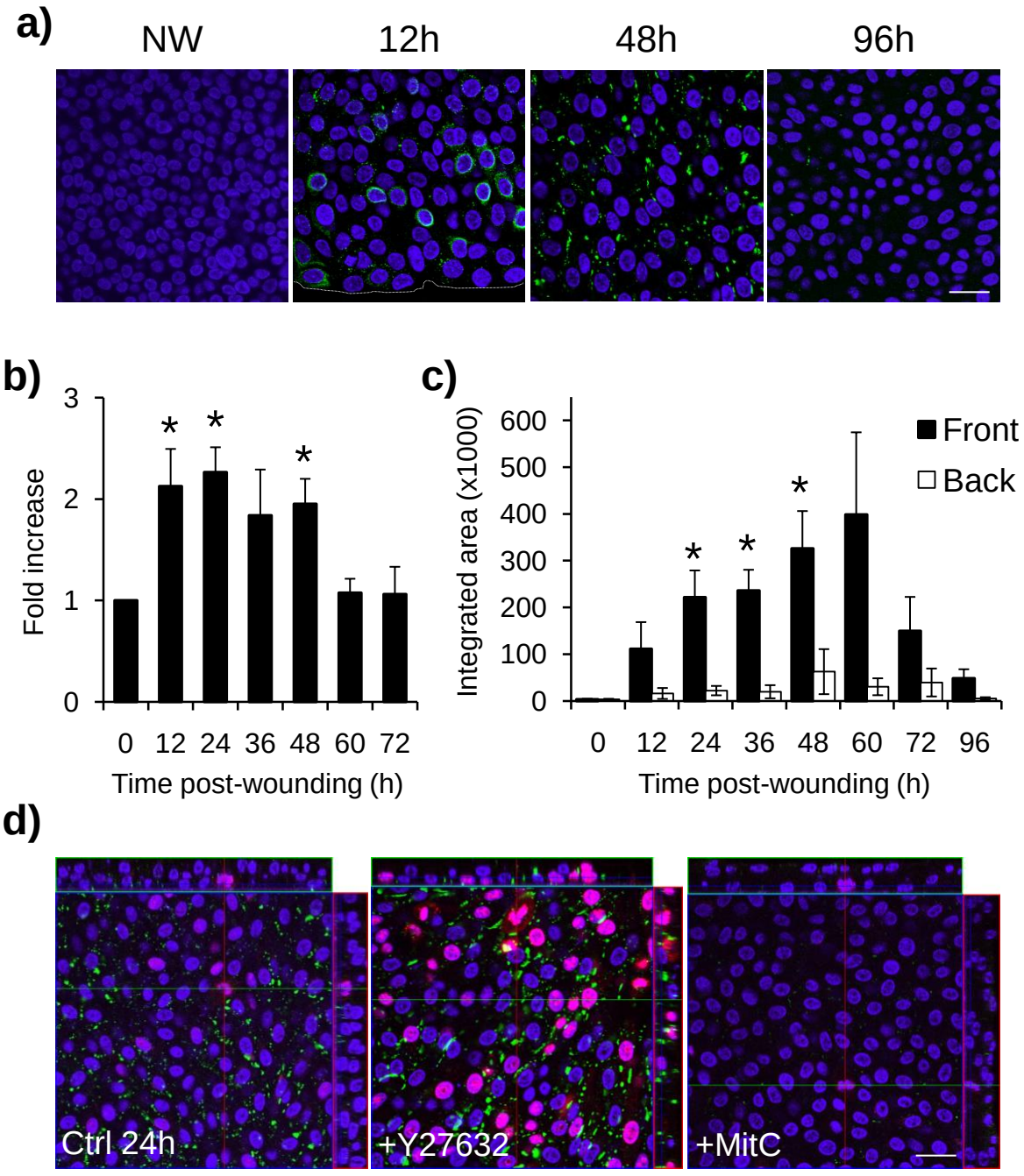
a)
NW
12h
48h
96h
b)
Fold increase
0
1
2
3
*
*
*
0 12 24 36 48 60 72
Time post-wounding (h)
c)
Integrated area (x1000)
0
100
200
300
400
500
600
*
*
*
Front
Back
0 12 24 36 48 60 72 96
Time post-wounding (h)
d)
Ctrl 24h
+Y27632
+MitC

Figure 2

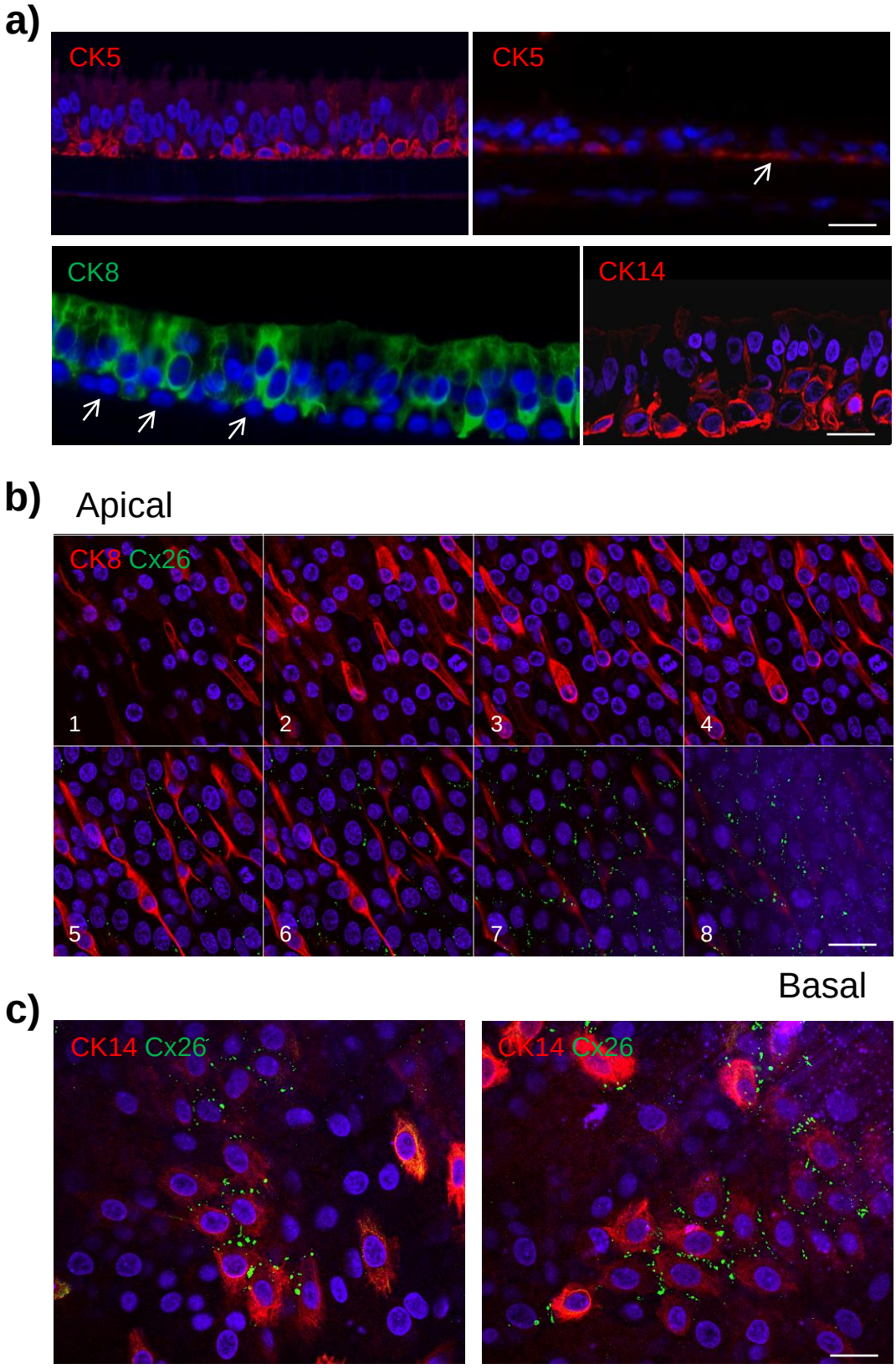
a)
CK5
CK5
CK8
CK14
b)
Apical
CK8 Cx26
1
2
3
4
5
6
7
8
Basal
c)
CK14 Cx26
CK14 Cx26

Figure 3

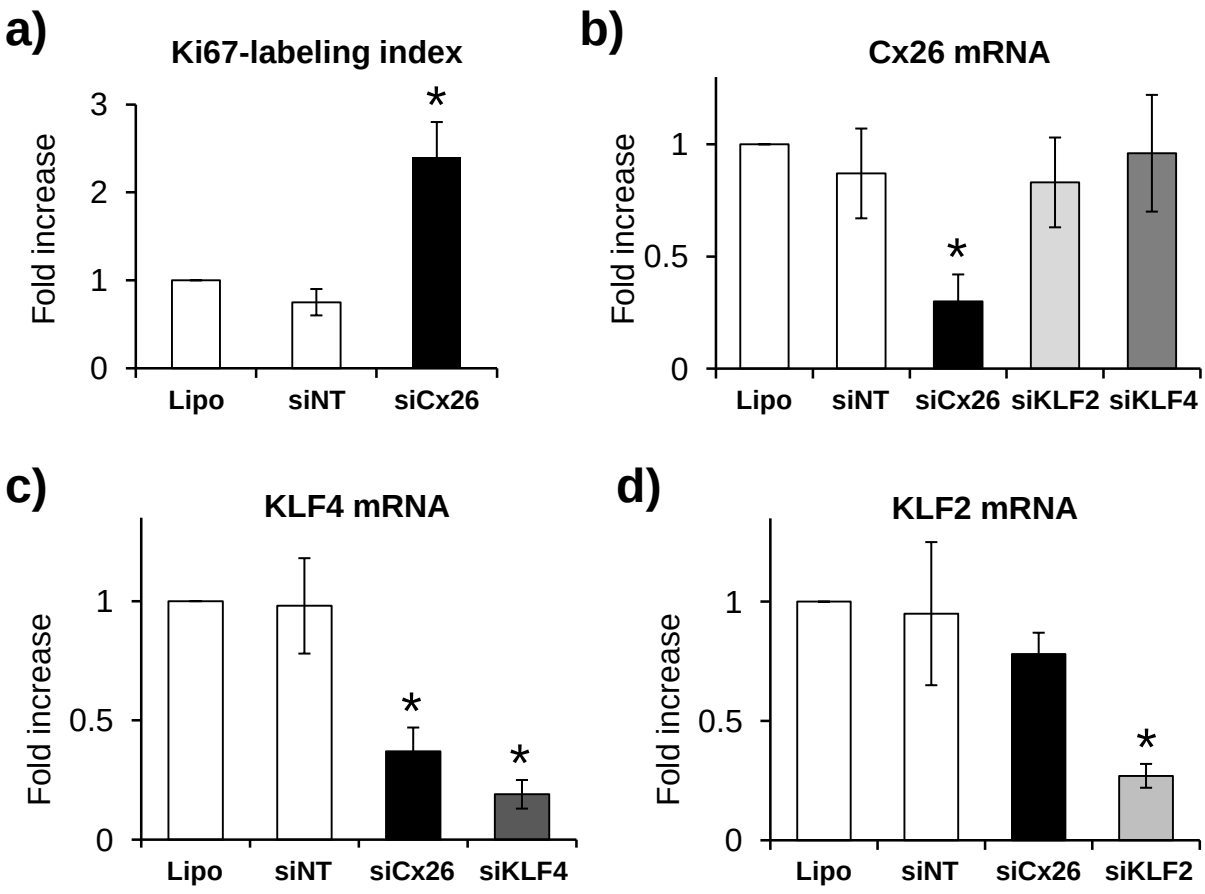
a)
Ki67-labeling index
Fold increase
3
2
1
0
*
Lipo
siNT
siCx26
b)
Cx26 mRNA
Fold increase
1
0.5
0
*
Lipo
siNT
siCx26
siKLF2
siKLF4
c)
KLF4 mRNA
Fold increase
1
0.5
0
*
*
Lipo
siNT
siCx26
siKLF4
d)
KLF2 mRNA
Fold increase
1
0.5
0
*
Lipo
siNT
siCx26
siKLF2

Figure 4

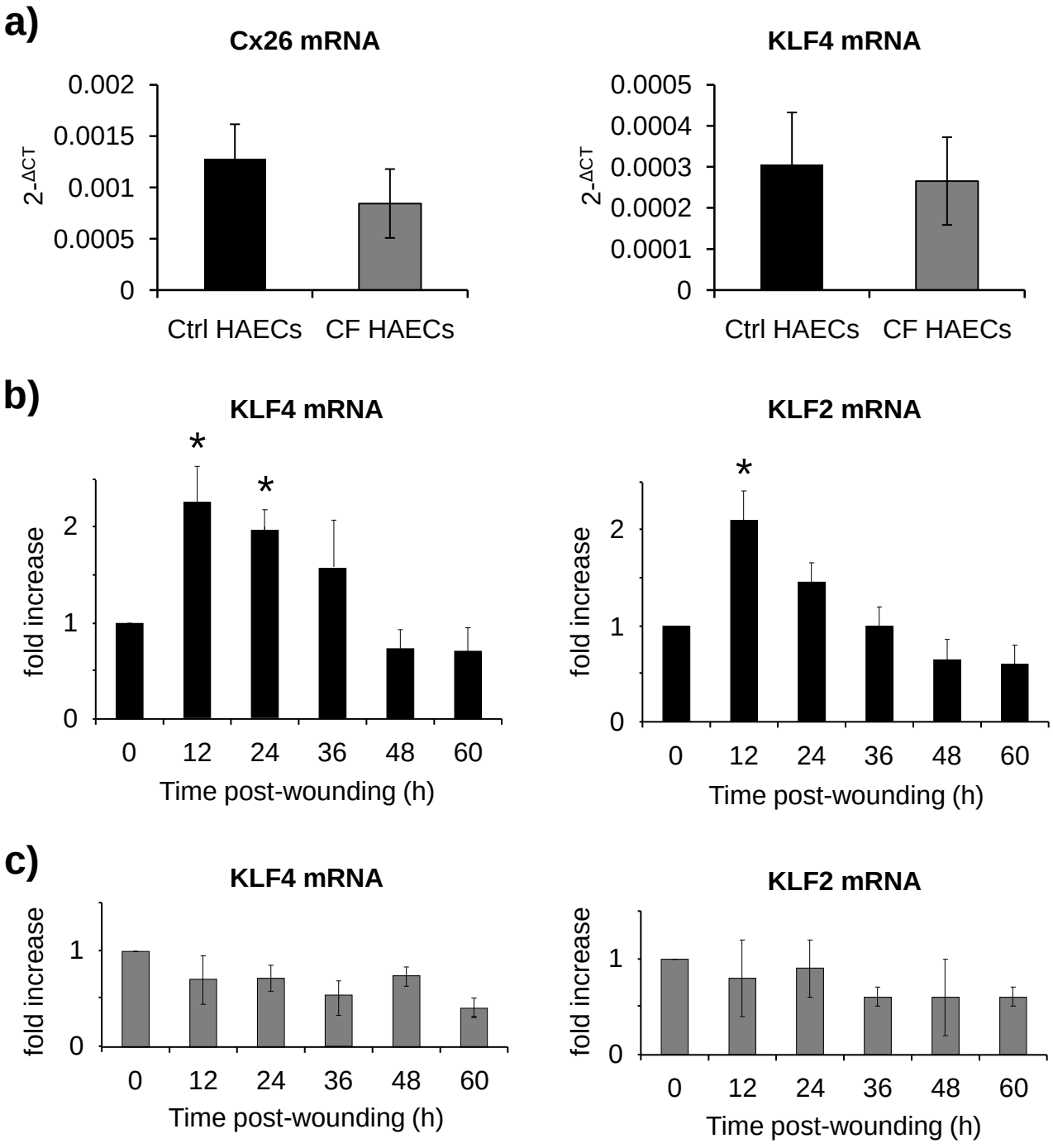
a)
Cx26 mRNA
0.002
0.0015
0.001
0.0005
0
2-ΔCT
Ctrl HAECs
CF HAECs
KLF4 mRNA
0.0005
0.0004
0.0003
0.0002
0.0001
0
2-ΔCT
Ctrl HAECs
CF HAECs
b)
KLF4 mRNA
*
*
fold increase
2
1
0
0
12
24
36
48
60
Time post-wounding (h)
KLF2 mRNA
*
fold increase
2
1
0
0
12
24
36
48
60
Time post-wounding (h)
c)
KLF4 mRNA
fold increase
1
0
0
12
24
36
48
60
Time post-wounding (h)
KLF2 mRNA
fold increase
1
0
0
12
24
36
48
60
Time post-wounding (h)

Figure 5

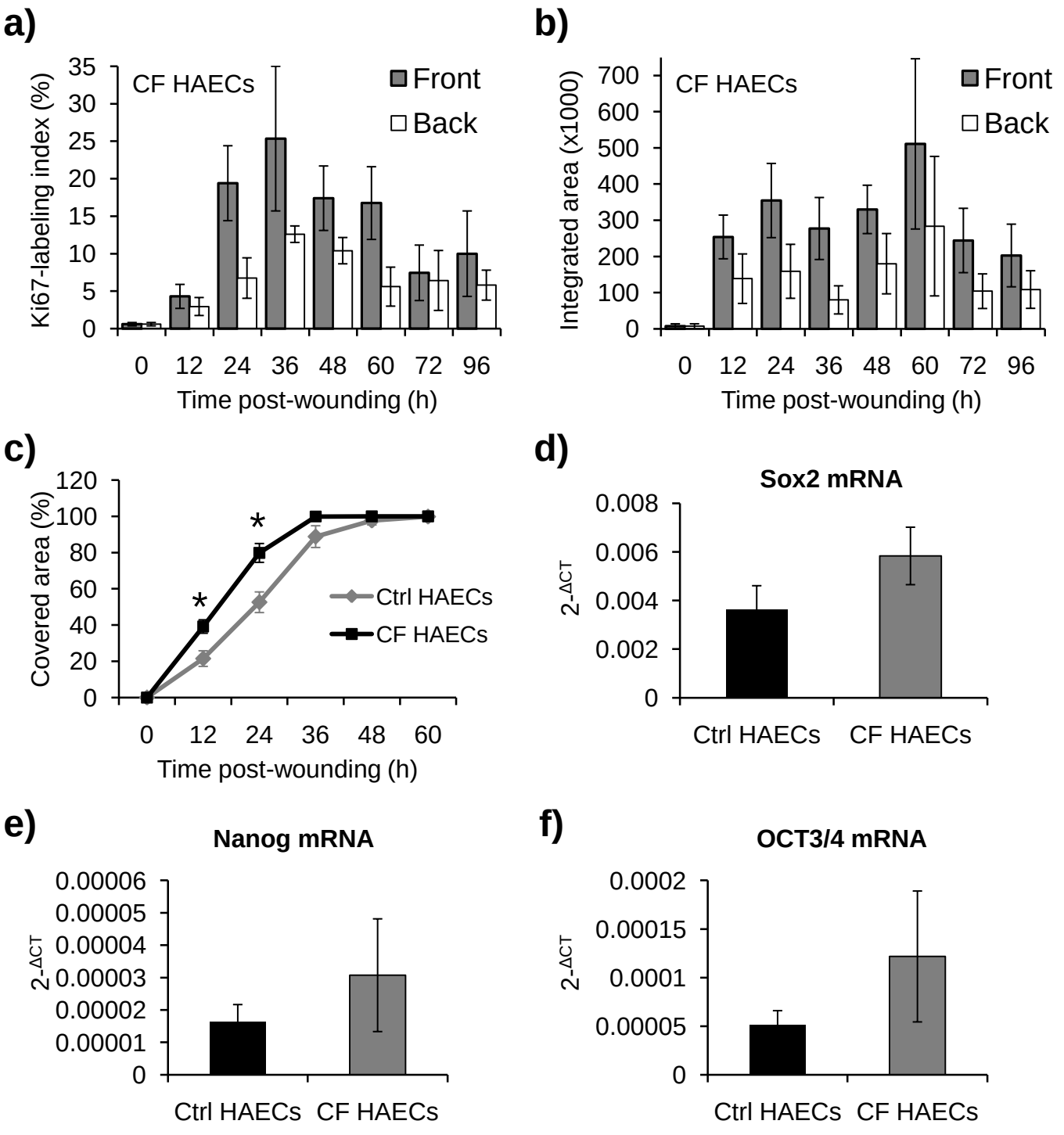
a)
CF HAECs
Front
Back
Ki67-labeling index (%)
0
5
10
15
20
25
30
35
0 12 24 36 48 60 72 96
Time post-wounding (h)
b)
CF HAECs
Front
Back
Integrated area (x1000)
0
100
200
300
400
500
600
700
0 12 24 36 48 60 72 96
Time post-wounding (h)
c)
Covered area (%)
0
20
40
60
80
100
120
*
*
Ctrl HAECs
CF HAECs
0 12 24 36 48 60
Time post-wounding (h)
d)
Sox2 mRNA
2-ΔCT
0
0.002
0.004
0.006
0.008
Ctrl HAECs
CF HAECs
e)
Nanog mRNA
2-ΔCT
0
0.00001
0.00002
0.00003
0.00004
0.00005
0.00006
Ctrl HAECs
CF HAECs
f)
OCT3/4 mRNA
2-ΔCT
0
0.00005
0.0001
0.00015
0.0002
Ctrl HAECs
CF HAECs

Figure 6

# Cx26 regulates proliferation of repairing basal airway epithelial cells

Crespin S[a], Bacchetta M[a], Bou Saab J[a], Tantilipikorn P[b], Bellec J[c], Dudez T[a], Nguyen T[c], Kwak BR[d], Lacroix JS[e], Huang S[f], Wiszniewski L[f], Chanson M[a]

*[a]Laboratory of Clinical Investigation III, Geneva University Hospitals and University of Geneva, Switzerland, [b]Mahidol University, Bangkok, Thailand, [c]INSERM UMR 1064, CHU Nantes, ITUN, Nantes, France, [d]Department of Pathology and Immunology, Department of Internal Medicine – Cardiology, University of Geneva, Switzerland, [e]Division of Otho-Rhino-Laryngology, Geneva University Hospitals, Geneva, Switzerland and [e]Epithelix Sàrl, Plan-les-Ouates, Switzerland*

**Running title:** Human airway epithelial cell repair

**Corresponding author:**

Marc Chanson PhD

Laboratory of Clinical Investigation III

Foundation for Medical Research

64 Avenue de la Roseraie

1205 Geneva 4

Tel. +41 22 37 24 611

Fax. +41 22 34 75 979

Email: marc.chanson@hcuge.ch

## Supplemental Methods and Materials

### Airway cell cultures

All experimental procedures were explained in full to subjects and all subjects provided written informed consent. The study was conducted according to the declaration of Helsinki on biomedical research (Hong Kong amendment, 1989) and received approval from our local Ethical Commission. Freshly dissociated HAECs were seeded onto porous Transwell inserts undercoated with a feeder layer of human airway fibroblasts and maintained at the air–liquid interface at 37°C in 5% $CO_2$ (Wiszniewski et al., 2006). This procedure generated well-differentiated pseudostratified airway epithelia which were used for experiments between 1-5 months of culture.

UNCN1T, UNCN2T and UNCN3T human bronchial epithelial cell lines (referred to as UNCN cells) are HAECs immortalized by introduction of Bmi-1 and the catalytic subunit of telomerase (hTERT) into primary bronchial cells (Fulcher et al., 2009).

### RNA Silencing and ReverseTranscription Polymerase Chain Reaction

Transfection of UNCN cells with siRNAs was performed for 6 hours with the use of lipofectamine® RNAiMAX (Invitrogen) and efficiency was determined 48 hours after transfection by RT-qPCR.

Primary HAECs were transduced with lentiviral vectors expressing a short hairpin RNA (shRNA) directed against Cx26 or a scramble sequence (shAlter). A GFP reporter gene expression cassette driven by the elongation factor 1 alpha (EF1-α) promoter was also contained in the vectors. Briefly, small interfering RNA (siRNA) sequences were embedded in the following short hairpin RNA (shRNA) structure: 5'–sense siRNA-TCAAGAG-antisense siRNA–3'. The siRNA sequences (Invitrogen) targeting Cx26 mRNA (5'–GCG CCT TAG GCA AAC TCC TTG ACA A–3'), and a scramble siRNA (siAlter) sequence (5'–

GAT AGA AAG GAT TGA CAG TGG TG– 3') were used to synthesize the shRNAs shCx26, shKLF4 and shAlter, respectively. The two sequences were cloned in a HIV-based lentiviral backbone (pLVTHM, kindly provided by Pr D. Trono, EPFL, Lausanne, Switzerland) downstream of the RNA polymerase III promoter H1. HIV-based lentiviral particles were produced using 293T cells as packaging cells. Lentiviral vector titers were determined by measuring GFP fluorescence by fluorescence activated cell sorting (FACS) in HeLa cells transduced with a serial dilution of the vectors.

Total cellular RNA was isolated from UNCN cells or HAECs with the RNEasy Minikit (Quiagen, Hombrechtikon, Switzerland) or the Ambion RNAqueous-Micro Kit (Life technologies, Zug, Switzerland). The Quantitect reverse transcription kit (Quiagen) was used to purify and reversely transcribed RNA in a Biometra thermocycler (Biolabo Scientific Instruments SA, Châtel-St-Denis, Switzerland), according to the manufacturer's instructions. For RT-PCR, cDNA was mixed with TaqMan Gene Expression Assay Mix containing forward and reverse primers for appropriate genes (Life Technologies, Zug, Switzerland). The PCR reaction was performed in triplicate on MicroAmp Fast Optical 96-Well Reaction Plate with Barcode (Life Technologies). Plates were read with StepOne thermocycler. The thermal cycle (CT) of each gene was detected and subtracted from the CT of 18S to obtain $\Delta$CT. All sample values were calculated according to the $2^{-2\Delta CT}$ or the $2^{-\Delta\Delta CT}$ algorithm (fold increase) when comparing relative changes (Schmittgen, Livak, 2008).

**Western Blotting and Immunohistochemistry**

Proteins were immunoblotted overnight at 4$^{o}$C with antibodies against Cx26 (Invitrogen). Anti-β-actin (clone AC-15, Sigma, St-Louis, MO) antibody was used to verify for equivalent protein loading. This step was followed by 1-hr incubation with goat anti-mouse or anti-rabbit IgG secondary antibodies conjugated to peroxidase (Jackson ImmunoResearch, Newmarket,

Suffolk, UK). Immunoreactivity was detected through the Super Signal West Pico kit (Pierce, Lausanne, Switzerland).

For immunostaining, fixed tissues/cells were incubated overnight at 4°C with rabbit antibodies against Cx26 and mouse antibodies against Ki-67, CK5 (Dako Cytomation, Blostrup, Denmark) or CK8 and CK14 (Abcam, Cambridge, UK). Cells were next incubated for 2 h at room temperature using Alexa 488-coupled goat anti-rabbit and Alexa 568-coupled goat anti-mouse antibodies (Molecular Probes Inc., Eugene, OR). In some experiments, rhodamine–phalloidin (Sigma, Steinheim, Germany) was used during the time of the secondary antibody incubation for staining actin cytoskeleton. DAPI (AppliChem, Darmstadt, Germany) was used for counterstaining nuclei. After rinsing, cells were mounted in Vectashield (Vector Laboratories, Burlingame, CA) before microscopic examination.

**Wound closure assay**

A 1-2 s air pulse of 0.1-0.5 bar was applied from a 4 mm distance to the airway epithelium cell surface (Crespin et al., 2011). The apical surface was then washed with a buffered saline solution, containing 0.9% NaCl supplemented with 10 mM HEPES and 1.25 mM $CaCl_2$, to remove debris and detached cells. No difference in the wounded areas was measured between Ctrl and CF HAEC cultures. The kinetic of wound closure was determined by image analysis. To this end, we used an automated inverted Leica DM IRE2 microscope equipped with a motorized DMSTC xy stage (Leica Microsystems, Heerbrugg, Switzerland) and a Nikon DS-5Mc digital camera (Nikon, Egg, Switzerland) connected to a personal computer. At regular intervals, the surface area of each insert was scanned using a 5x objective. Reconstitution of the culture surface was performed with the Image Pro Plus 6.0 software (MediaCybernetics, Bethesda, MD).

**Microscopic examination**

Stained tissues/cells were viewed on an inverted TMD300 microscope (Nikon) equipped with a CoolSnap $HQ^2$ CCD camera (Visitron Systems GmbH, Puchheim, Germany) or an inverted Zeiss LSM510 laser scanning confocal microscope (Carl Zeiss, Feldbach, Switzerland). Images acquired through a 40x or a 63x oil immersion objective were further processed using LSM Image Browser (Carl Zeiss, Inc.) or Metafluor® 7.7.4.0 (Visitron Systems) and Adobe Photoshop CS2 9.0 (Adobe Systems Incorporated, San Jose,CA, USA). Whole surface scanning of cell samples was also realized with a Mirax Micro digital slide scanner (Carl Zeiss). Quantification of immunostaining was performed with MetaMorph® 6.0 (Visitron System) or Image J (http://rsb.info.nih.gov/ij/). Threshold to separate quantifying signals from background was manually determined in each image from the distribution of the intensity of the fluorescent signal provided by the software. For quantification, 5 images (689x412 pixels) was taken (x20x) at the back and front area for each Transwell filters and the number of Ki67-postive cells, the number of DAPI-stained nuclei and the integrated area value of the Cx26 signal was determined. This allowed calculating in each Transwell filter the Ki67-labeling index and the amount of Cx26 signal in the back and front area by averaging values obtained from the 5 images. This method was applied to series of Transwell filters in HAECs obtained from different donors/patients before (time 0h) and for different times after wounding.

## References

Crespin S, Bacchetta M, Huang S, et al. Approaches to study differentiation and repair of human airway epithelial cells. Methods Mol Biol 2011;742:173-85.

Fulcher ML, Gabriel SE, Olsen JC, et al. Novel human bronchial epithelial cell lines for cystic fibrosis research. Am J Physiol Lung Cell Mol Physiol 2009;296:L82-L91.

Schmittgen TD, Livak KJ. Analyzing real-time PCR data by the comparative Ct method. Nature Protocols 2008;3:1101-1108.

Wiszniewski L, Jornot L, Dudez T, et al. Long-term cultures of polarized airway epithelial cells from CF patients. Am J Respir Cell Mol Biol 2006;34:39-48.

## Supplemental Figure legends

**Supplemental Figure 1: a)** A representative field of repairing HAECs co-immunostained for Cx26 (green) and Ki67 (red) 24h after wounding. Cx26 was detected at junctional areas between Ki67-positive cells (green circle) and Ki67-negative cells (blue circle). Ki67-positive cells but negative for Cx26 (red circle) were also detected. **b)** Two representative x-z projections of confocal images of HAEC cultures co-immunostaining for Cx26 (green) and Ki-67 (red) 24h after wounding. Cx26 was detected around Ki67-positive cells (open arrows) and Ki67-negative cells (closed arrows). Nuclei were stained with DAPI (blue). Bar=100 μm in **a)** and 25 μm in b).

**Supplemental Figure 2: a)** Confocal image of UNCN2T cells immunostained for Cx26 (green). Actin was stained with phalloidin (red) and nuclei with DAPI (blue). Bar = 25 μm. **b)** Western blot for Cx26 in total protein obtained from UNCN1T, UNCN2T and UNCN3T cells. *β*-actin was used as a control for protein loading. **c)** The expression of Cx26 at the junctional membrane of UNCN1T, UNCN2T and UNCN3T cells was reduced after transfection with 3 different siRNAs against Cx26 as well as with a mix of the 3 (siRNAMix). Values (integrated area) were normalized to the expression levels measured in cells treated with lipofectamine (Lipo) only. siNT represents Cx26 expression in cells treated with a non-targeting (NT) siRNA.

**Supplemental Figure 3:** Ki67 expression in non-CF and CF HAECs in response to wounding. Representative images of Ki67 immunostaining (red) are shown on control (Ctrl HAECs) and CF HAECs cultures 24, 36 and 48h post-wounding. The dotted line in some images delineates the denuded area. Note the disorganized Ki67 staining in CF HAECs as compared to Ctrl HAECs.

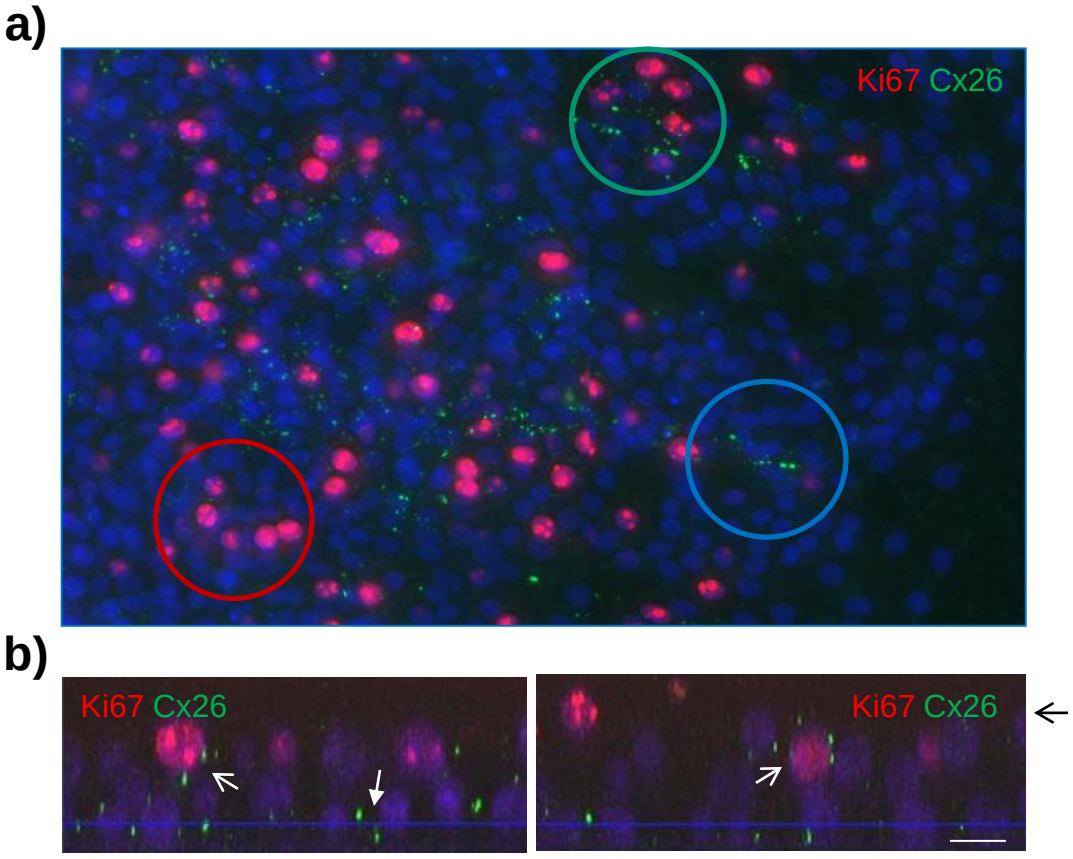


Supplemental fig. 1

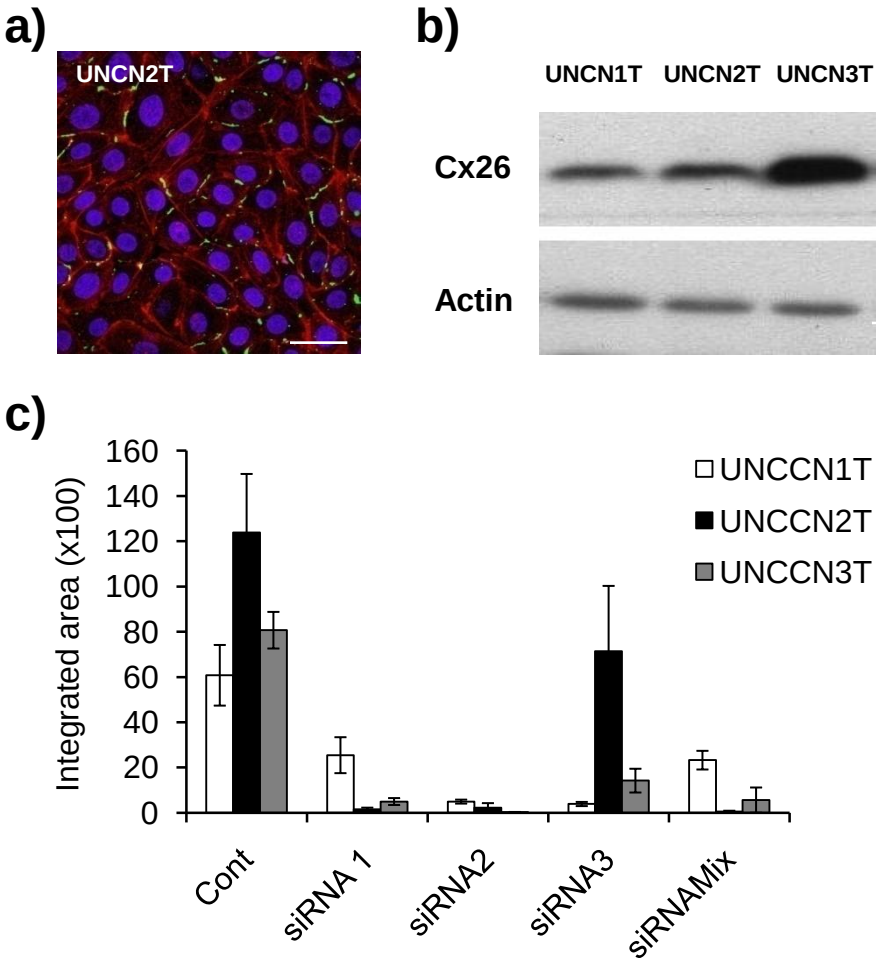


Supplemental fig. 2

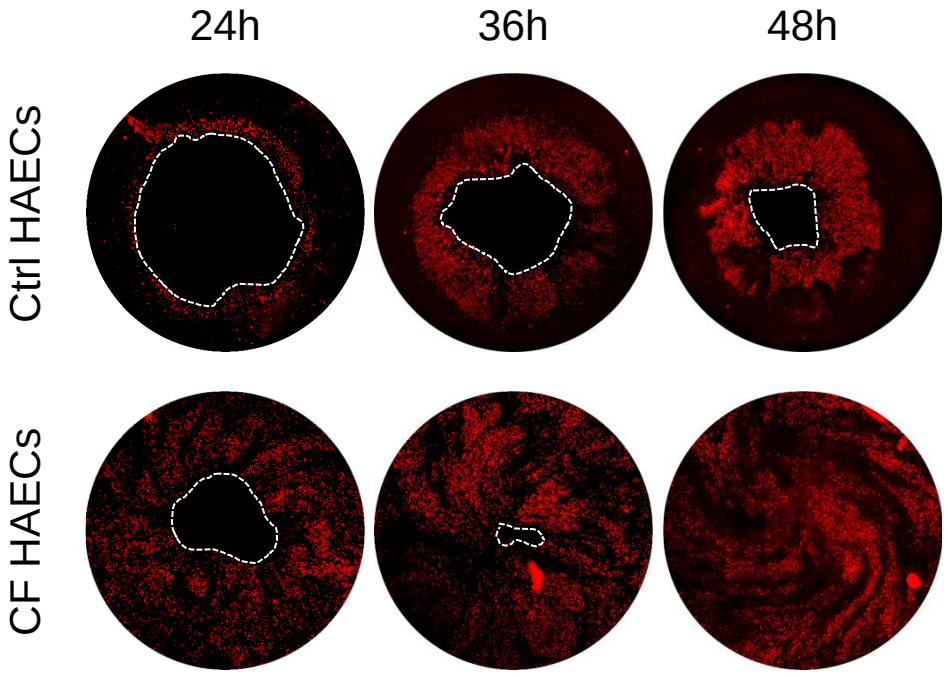


Supplemental fig. 3